

# Novel Emitting System Based on a Multifunctional Bipolar Phosphor: An Effective Approach for Highly Efficient Warm-White Light-Emitting Devices with High Color-Rendering Index at High Luminance

Mingxu Du, Yansong Feng, Dongxia Zhu, Tai Peng, Yu Liu,\* Yue Wang,\* and Martin R. Bryce\*

White organic light-emitting diodes (OLEDs) are a very promising technology for next-generation solid-state lighting.<sup>[1]</sup> High-quality illumination sources require white OLEDs (WOLEDs) with a high color-rendering index (CRI) of >80.<sup>[1c]</sup> Although some two-color WOLEDs produced by an orange or yellow emitter complemented with a blue emitter, exhibit impressive electroluminescence (EL) efficiency, they have low CRI ( $\leq 70$ ).<sup>[2]</sup> Therefore, three-color (red, green, and blue) or more emitters are a prerequisite for high CRI.<sup>[3]</sup> Today, WOLEDs based on phosphorescent emitters with the CRI  $\geq 80$ <sup>[4]</sup> have achieved rather high external quantum efficiency (EQE) of  $\geq 20\%$  owing to near 100% internal quantum efficiency of electrophosphorescence. However, they show only moderate peak power efficiencies (PEs) ( $40\text{--}60 \text{ lm W}^{-1}$ ) and suffer from a pronounced efficiency roll-off: PEs at the luminance of  $1000 \text{ cd m}^{-2}$  required for lighting applications generally reach only  $\leq 45 \text{ lm W}^{-1}$  WOLEDs,<sup>[5,6]</sup> which is below that of fluorescent tubes ( $60\text{--}70 \text{ lm W}^{-1}$ ).<sup>1c</sup> The PE is limited by the fact that singlet and triplet excitons generated on the large gap host material inevitably lose energy upon their transfer to the guest emitters.<sup>[4a]</sup> Thus, there is a need for conceptually new emitting systems, where the excited state energy will more efficiently transfer from the higher energy (blue and/or green) to the lower energy (yellow and/or red) emitters with little power

losses due to a suitable  $\Delta E_T$  ( $\leq 0.3 \text{ eV}$ ) between the respective host and guest. Employing as few as possible components in the emitting system of WOLEDs is a means to reduce the energy losses through the simplified exciton-formation and energy-transfer processes. For achieving this, appropriate multifunctional emitter molecules are needed combined with a smart device design strategy.

A few efficient phosphorescent OLEDs (PhOLEDs) have been reported based on phosphorescent hosts.<sup>[7a,d]</sup> These non-fluorescent-host emitting systems are promising to simplify/optimize the electrophosphorescent process.<sup>[7]</sup> However, until now, integrating such an advanced doping model into the construction of the WOLEDs has not yet been achieved. In this work, three emitting complexes originating from our group: bis(2-(2-hydroxyphenyl)-pyridine)beryllium (Bepp<sub>2</sub>,  $\lambda_{\text{max}} \approx 450 \text{ nm}$ ),<sup>[8]</sup> bis(4,6-di-fluorophenyl)pyridinato-*N,C*'<sup>2</sup>iridium(III) *N,N'*-diisopropyl-carbazol-9-yl-amidine (FPPCA,  $\lambda_{\text{max}} \approx 500 \text{ nm}$ ), and bis(7,8-benzoquinolino)iridium(III) *N,N'*-diisopropyl-diisopropyl-guanidinate (BZQPG,  $\lambda_{\text{max}} \approx 605 \text{ nm}$ ),<sup>[9]</sup> which could provide essential colors of blue (B), green (G), and orange-red (OR), respectively, for white light, were well organized for realizing a simplified WOLED composed of two adjacent G-OR (FPPCA:BZQPG) and B-G (Bepp<sub>2</sub>:FPPCA) emitting layers (EMLs). In this strategy, phosphorescent (P) molecule FPPCA was distributed through both EMLs and showed an unprecedented multifunctional property by playing four key roles: (i) the charge-transporting host, (ii) the green emitting host, (iii) the sensitizer for the dopant P molecule BZQPG in the G-OR layer, and (iv) the green dopant emitter in the B-G layer. This new method endowed the device with the advantage of a reduced number of constituent components and EMLs, which allows for a simplified fabrication processes and effectively reduces structural heterogeneity. Furthermore, careful manipulation for the well-matched FPPCA:BZQPG combination utilizes all the electrically generated excitons in the phosphor-phosphor type (PPT) G-OR layer, where the bipolar character of FPPCA results in a wide emission zone to enhance carrier and exciton utilization, thereby dominating the high electrophosphorescent efficiency. Meanwhile, the fluorescent (F) molecule Bepp<sub>2</sub> is used to generate blue singlet emission in the B-G layer and served as a host for sensitizing green emission, thereby achieving the broad white EL spectrum. An optimal management of B-G and G-OR layers aiming at balanced charge injection together with simultaneous efficient charge/exciton confinement, ensured this three-color device possesses stable and high EL performance

Dr. M. X. Du, Y. S. Feng, T. Peng, Prof. Y. Liu, Y. Wang  
State Key Laboratory of Supramolecular  
Structure and Materials  
Jilin University  
Changchun 130012, P. R. China  
E-mail: yuliu@jlu.edu.cn; yuewang@jlu.edu.cn



Prof. D. X. Zhu  
Institute of Functional Material Chemistry  
Faculty of Chemistry  
Northeast Normal University  
Renmin Road 5268, Changchun, Jilin 130024, P. R. China

Prof. M. R. Bryce  
Department of Chemistry  
Durham University  
Durham, DH1 3LE, UK  
E-mail: m.r.bryce@durham.ac.uk

This is an open access article under the terms of the Creative Commons Attribution License, which permits use, distribution and reproduction in any medium, provided the original work is properly cited.

The copyright line for this article was changed on 20 Sept 2016 after original online publication.

DOI: 10.1002/adma.201600451

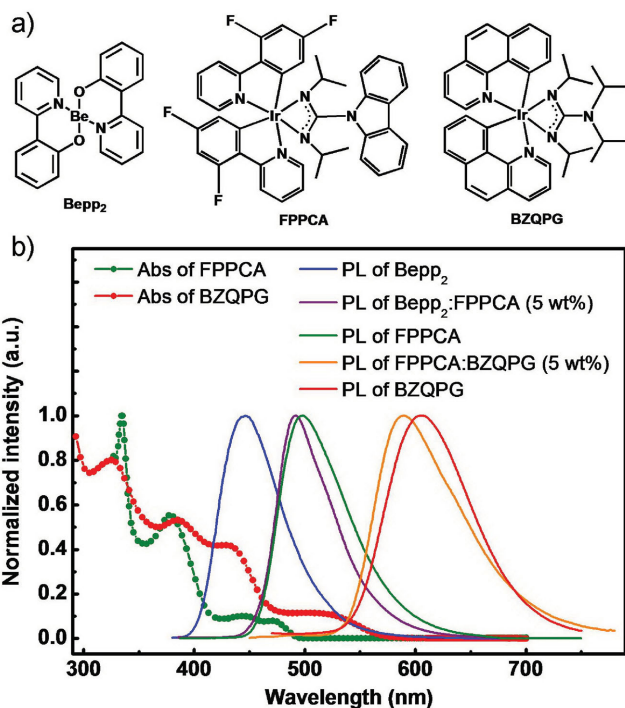


**Figure 1.** a) Molecular structures of Bepp<sub>2</sub>, FPPCA, and BZQPG. b) UV-vis absorption of FPPCA and BZQPG in neat thin film and PL spectra of neat films of Bepp<sub>2</sub>, FPPCA, and BZQPG, and the films of FPPCA and BZQPG doped in Bepp<sub>2</sub> and FPPCA, respectively, with 5 wt% doping concentration.

as follows: very high forward-viewing EQE of 27.3% and PE of 74.5 lm W<sup>-1</sup> at an illumination-relevant luminance of 1000 cd m<sup>-2</sup> with a high CRI of 85 and desirable eye-friendly warm-white<sup>[5c,10]</sup> Commission Internationale de L'Eclairage (CIE<sub>x,y</sub>) coordinates of (0.43, 0.46) were realized, which maintained the high levels of 26.3% and 56.5 lm W<sup>-1</sup> at 5000 cd m<sup>-2</sup>, 24.3% and 45.8 lm W<sup>-1</sup> at the extremely high luminance of 10 000 cd m<sup>-2</sup>, with CRI in the range 86–87. To our knowledge, these values are competitive with, and even exceed, the best published data for a WOLED,<sup>[2,4–6]</sup> simultaneously exhibiting a high efficiency and high CRI based on high luminance for the practical solid-state lighting.

**Figure 1a,b** shows the chemical structures of Bepp<sub>2</sub>, FPPCA, and BZQPG and the absorption and photoluminescence (PL) spectra in neat films. The spectral overlap between the fluorescence of Bepp<sub>2</sub> ( $\lambda_{\text{max}} \approx 450$  nm) and the absorption spectrum of FPPCA, and between the phosphorescence of FPPCA ( $\lambda_{\text{max}} \approx 500$  nm) and the absorption of BZQPG, enables effective energy transfer from Bepp<sub>2</sub> to FPPCA, and/or from FPPCA to BZQPG. Accordingly, the PL spectra of doped Bepp<sub>2</sub>:FPPCA (D) and FPPCA (H):BZQPG thin films with a low concentration of 5 wt%, show emission only from FPPCA (D) at  $\lambda_{\text{max}} \approx 495$  nm and BZQPG at  $\lambda_{\text{max}} \approx 590$  nm: quantum yields are 0.85 ± 0.03 and 0.62 ± 0.03, with phosphorescence lifetimes of 0.68 and 1.22 μs, respectively (Figure S1, Supporting Information). Such high yields and short lifetimes are beneficial for high EL efficiency and reduced roll-off.<sup>[11]</sup> Moreover, the triplet energy alignment of 2.6, 2.4, and 2.1 eV for Bepp<sub>2</sub>, FPPCA, and BZQPG, respectively,<sup>[8,9]</sup> indicated that both triplet energy

transfer processes are sufficient and losses are minimal due to their appropriate  $\Delta E_{\text{T}}$  (0.2–0.3 eV).

Time-of-flight measurements revealed that FPPCA and BZQPG are bipolar molecules with comparable hole and electron mobility as high as 10<sup>-3</sup> cm<sup>2</sup> V<sup>-1</sup> s<sup>-1</sup>,<sup>[9]</sup> while Bepp<sub>2</sub> is an electron-transporting molecule due to its high electron mobility of 1.3 × 10<sup>-3</sup> cm<sup>2</sup> V<sup>-1</sup> s<sup>-1</sup>. The single-carrier devices based on active layers of FPPCA (*x* nm)/Bepp<sub>2</sub> (*y* nm) (*x* + *y* = 30 nm) with the configurations of indium tin oxide (ITO)/1,3,5-tris(*N*-phenylbenzimidazol-2-yl)benzene (TPBi) (10 nm)/active layer (30 nm)/LiF/Al (electron-only device) and ITO/active layer (30 nm)/4,4'-bis(*N*-(1-naphthyl)-*N*-phenylamino)biphenyl (NPB) (10 nm)/Al (hole-only device) were fabricated, where ITO and LiF/Al are the anode and the cathode, respectively; TPBi and NPB layers prevent injection of holes and electrons from the anode and cathode, respectively.<sup>[12]</sup> The current density (*J*) versus voltage (*V*) curves are shown in **Figure 2a**. For electron-only devices, the *J*-*V* characteristics are almost independent of the relative layer thicknesses, suggesting both molecules possess comparable electron-transporting properties. In contrast, in the hole-only devices the current decreases with increasing relative thickness of Bepp<sub>2</sub> at a constant driving voltage. This indicates that Bepp<sub>2</sub> has relatively weak hole transporting ability compared with FPPCA, which is in accord with the electron-transporting nature of Bepp<sub>2</sub>.<sup>[8]</sup>

The recombination zone in the FPPCA- and Bepp<sub>2</sub>-based EMLs was further confirmed as follows. Four devices with a uniform configuration of ITO (100 ± 2 nm)/NPB (35 nm)/EML (30 nm)/TPBi (30 nm)/LiF (0.5 nm)/Al were fabricated by introducing a thin layer (2 nm) of BZQPG (5 wt%) doped in FPPCA, and FPPCA (5 wt%) doped in Bepp<sub>2</sub> into different zones in the EML of the respective devices: namely devices F10 and F20 (F-series) based on FPPCA, and Be10 and Be20 (Be-series) based on Bepp<sub>2</sub> (Figure 2b). Here, NPB and TPBi are the hole-transporting layer (HTL) and the electron-transporting layer (ETL), respectively. The EL spectra at a luminance of 1000 cd m<sup>-2</sup> are shown in Figure 2c. In the F-series devices, the EL is almost independent of the different zone in the doping layer, where the relative intensities of the host FPPCA green emission and the dopant BZQPG orange-red emission are comparable. This demonstrates that both the holes and the electrons migrate freely and the excitons form and diffuse throughout the EMLs based on FPPCA host, rendering the FPPCA molecules bipolar. Be10 and Be20 showed different EL spectra: two emission peaks from the dopant FPPCA and the host Bepp<sub>2</sub>, respectively, are exhibited in Be10, whereas Be20 shows a slight green shoulder from the dopant, along with dominant blue emission from the host, indicating that the recombination region of electrons and holes in the Bepp<sub>2</sub> layer is close to the NPB/Bepp<sub>2</sub> interface and its optimized thickness is as narrow as ≈10 nm.

Based on the above characteristics, an optimized highly efficient three-color (OR-G-B) WOLED (Device 1) was obtained with a simple double-EML structure of ITO/NPB (35 nm)/FPPCA:BZQPG (0.8 wt%, 20 nm)/Bepp<sub>2</sub>:FPPCA (1.5 wt%, 10 nm)/TPBi (30 nm)/LiF (1 nm)/Al (Figure S2, Supporting Information). Here, a novel PPT host-guest system contributed to G-OR EL, and an adjacent classical fluorophor-phosphor type (FPT) layer gave B-G EL, without any interlayer. **Figure 3a**

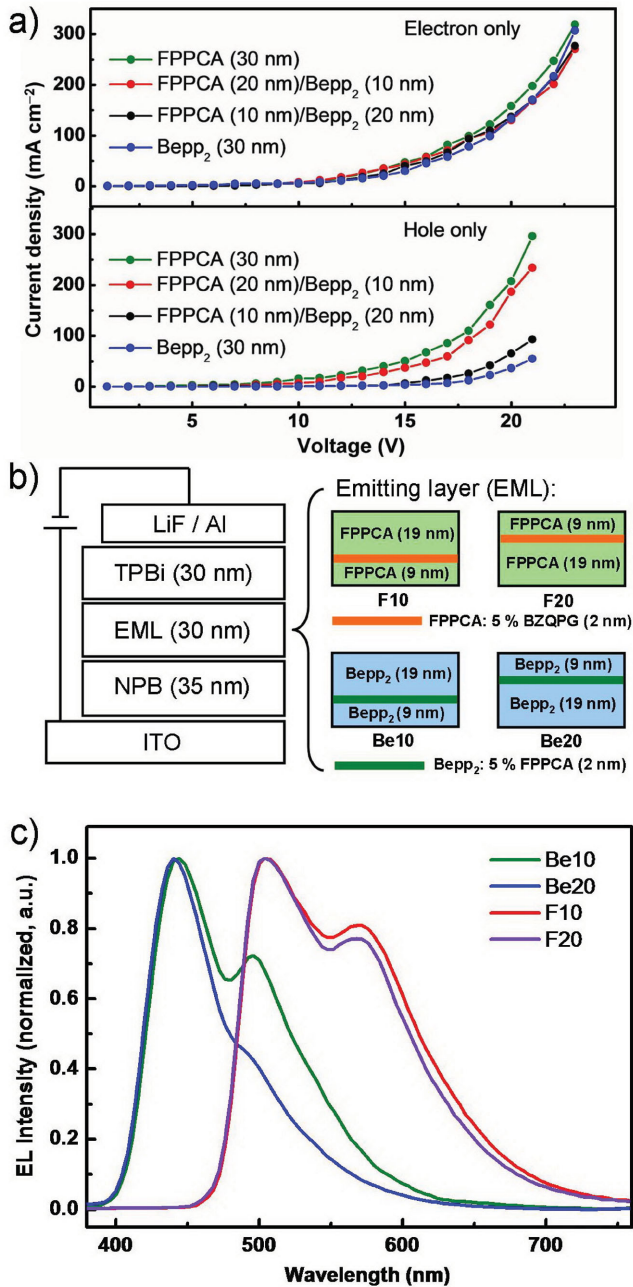


**Figure 2.** a) Current density–voltage curves of the electron-only and hole-only devices with the active layers of FPPCA ( $x$  nm)/Bepp<sub>2</sub> ( $y$  nm) ( $x + y = 30$  nm). b) Schematic structures of the devices of Be10, Be20, F10, and F20. c) EL spectra of Be10, Be20, F10, and F20 at the luminance of 1000 cd m<sup>-2</sup>.

shows the proposed energy diagram of Device 1. Theoretically, both singlet and triplet excitons are created with a ratio of 1:3 in either of the EMLs.<sup>[13]</sup> In the FPPCA:BZQPG layer, all the generated excitons can produce either green emission through direct radiative decay on the host FPPCA molecule or orange-red emission from the dopant BZQPG molecules through host–guest energy transfer. In another EML, the Bepp<sub>2</sub> molecules not only generate blue singlet emission but also sensitize

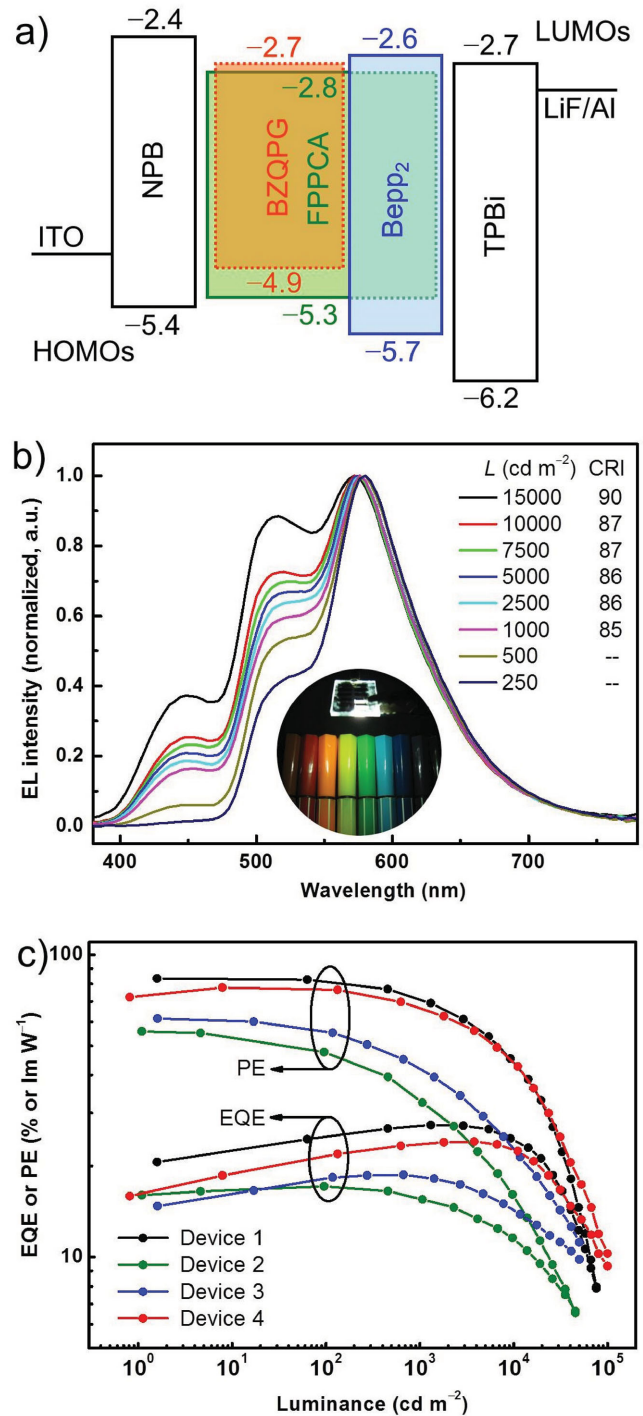


**Figure 3.** a) Proposed energy diagram of the materials used in OLEDs. b) EL spectra of Device 1 at different luminances ( $L$ ). Inset: A photograph of Device 1 illuminating at 10 000 cd m<sup>-2</sup> with a CRI of 87. c) PE–luminance ( $L$ )–EQE curves of Devices 1, 2, 3, and 4.

the emission of FPPCA in both EMLs, leading to the increase in total green emission intensity.

Figure 3b,c shows the important EL characteristics. The data in Table 1 show driving voltages of 3.8, 4.9, and 5.6 V for luminances of 1000, 5000, and 10 000 cd m<sup>-2</sup>, respectively. Figure 3b

**Table 1.** Summary of EL performance for Devices 1, 2, 3, and 4.

Device	$V_{on}^a$ [V]	$V^b$ [V]	$\eta_p^b$ [ $\text{lm W}^{-1}$ ]	$\eta_{ext}^b$ [%]	CIE $_{x,y}^b$
Device 1	2.5	3.8, 4.9, 5.6	74.5, 56.5, 45.8	27.3, 26.3, 24.3	(0.43, 0.46), (0.42, 0.45), (0.41, 0.45)
Device 2	2.4	4.0, 5.2, 6.1	32.4, 21.2, 16.0	15.5, 13.1, 11.5	(0.24, 0.48), (0.23, 0.42), (0.22, 0.36)
Device 3	2.6	4.7, 6.1, 6.9	42.8, 28.6, 22.6	18.4, 16.1, 14.2	(0.21, 0.32), (0.20, 0.29), (0.19, 0.27)
Device 4	2.3	3.7, 4.7, 5.4	67.7, 53.2, 43.6	23.5, 24.0, 22.8	(0.53, 0.46), (0.51, 0.46), (0.51, 0.45)

<sup>a</sup>) Applied voltage required to reach a luminance of  $1 \text{ cd m}^{-2}$ ; <sup>b</sup>) Values at 1000, 5000, and 10 000  $\text{cd m}^{-2}$ , respectively.

shows warm-white EL due to the simultaneous fluorescent blue from Bepp<sub>2</sub> ( $\approx 450 \text{ nm}$ ), and phosphorescent green and orange-red from FPPCA ( $\approx 510 \text{ nm}$ ) and BZQPG ( $\approx 580 \text{ nm}$ ), respectively. The corresponding CIE $_{x,y}$  coordinates are (0.43, 0.46) at  $1000 \text{ cd m}^{-2}$  and (0.35, 0.44) at  $15\,000 \text{ cd m}^{-2}$ . This is due to the deeper HOMO (highest occupied molecular orbital) of Bepp<sub>2</sub> compared to FPPCA (Figure 3a) which produces an energy barrier ( $\approx 0.4 \text{ eV}$ ) when the holes inject from the G-OR layer into the B-G layer. Moreover, the creation of blue singlet excitons on Bepp<sub>2</sub> also needs a certain voltage.<sup>[6a]</sup> Thus, with the increased driving voltage, both the fluorescent blue and the phosphorescent green emission steadily increase compared to the orange-red emission. At a luminance of  $1000 \text{ cd m}^{-2}$ , the WOLEDs have the PE and EQE values of  $74.5 \text{ lm W}^{-1}$  and 27.3%, respectively. The efficiency roll-off is low. At  $5000 \text{ cd m}^{-2}$ , which is a critical level for solid-state lighting,<sup>[5c]</sup> the PE and EQE remain as high as  $56.5 \text{ lm W}^{-1}$  and 26.3%, respectively, with CRI of 86. Even at 10 000 and 15 000  $\text{cd m}^{-2}$ , high PEs ( $45.8$  and  $38.5 \text{ lm W}^{-1}$ ) and EQEs (24.3 and 22.1%) are maintained. Lighting sources are generally characterized by their total emitted light, which is a factor of 1.7–2.3 times more than the forward viewing efficiencies.<sup>[1a]</sup> Therefore, the present device should have total PE and EQE values approaching  $100 \text{ lm W}^{-1}$  and 50%, respectively, at  $5000 \text{ cd m}^{-2}$ , which are also the highest levels reported for WOLEDs with extra out-coupling and/or multilayer tandem structures,<sup>[14]</sup> as well as comparable to the most efficient lighting technologies.<sup>[15]</sup>

To elucidate the origin of the high performance of the Device 1, three reference devices (Devices 2, 3, and 4) with the same configuration as Device 1 were fabricated by using double neat films of FPPCA (20 nm)/Bepp<sub>2</sub> (10 nm) and a single doping film of Bepp<sub>2</sub>:FPPCA (D) (1.5 wt%, 30 nm) and FPPCA (H):BZQPG (0.8 wt%, 30 nm) as the EML, respectively (see Figure S2, Supporting Information). The efficiency-luminance (PE/EQE-L) characteristics of Devices 2, 3, and 4 and their EL spectra at different luminances (1000, 2500, and  $5000 \text{ cd m}^{-2}$ ) are shown in Figure 3c and 4. The two emission peaks in Device 2 are assigned to (i) direct exciton generation on the Bepp<sub>2</sub> and FPPCA molecules in the respective EML and (ii) singlet/triplet excited state energy in the blue EML transferring to the green EML; these are similar to those of Device 1 (Figure 3b) where both low-content dopants have almost no effect on the inherent properties of the host of Bepp<sub>2</sub> and FPPCA. Devices 3 and 4 comprise EMLs with the same doping concentration as the B-G and G-OR layers in Device 1 which could generally reflect the EL processes that occur within the two EMLs in Device 1.

In the EL spectra of Devices 3 and 4, the emission peaks originating from both the host and dopant molecules are observed,

due to suppression of energy transfer of singlet/triplet excitons at such low doping concentrations as 0.8 or 1.5 wt%. We attribute the increase of EQE for the white Device 1 on shifting from low to high luminance to the following reasons: (1) the shorter emission wavelength of blue and/or green color results from the larger energy gaps compared to orange or red; therefore, increasing the driving voltage leads to more blue and/or green excitons, which in turn leads to the high EQE at high luminance. (2) The recombination zone consisting of double EMLs without an interlayer in Device 1, which could induce the undesirable charge accumulation as well as the subsequent triplet-polaron and/or polaron-polaron quenching, allows all the excitons to decay radiatively and is key to maximizing the overall quantum efficiency of the device. (3) The bipolar phosphor molecule FPPCA which is distributed through both EMLs has different roles and is the essential feature for maximizing the overall quantum efficiency, especially retaining the high EQE at high luminance.

With increasing luminance as the driving voltage increased, the relative intensity of blue emission in Devices 2 and 3 also increased. This strongly supports the hypothesis for Device 1, namely that higher voltages favor the injection of holes into the B-G layer, which facilitates the creation of more blue excitons from Bepp<sub>2</sub>. For Device 4, increasing the voltage leads to gradually increased relative intensity of green emission indicating that the green excitons are not all captured by the BZQPG molecules and they decay radiatively. Such an EL process should exist in the G-OR layer in Device 1 with the same PPT system,

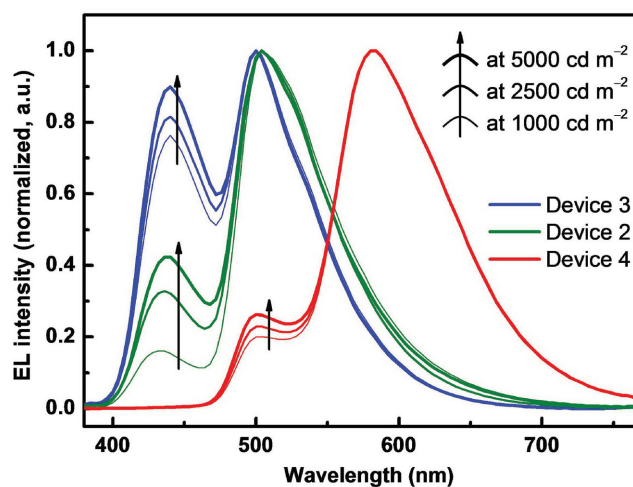


**Figure 4.** EL spectra of Devices 2, 3, and 4 at the luminance of 1000, 2500, and  $5000 \text{ cd m}^{-2}$ .

where the enhancement of green emission is likely to cause the EL spectral variation with changing voltage.

The comparable high EL data of both Devices 1 and 4 (Table 1 and Figure 3c) over the whole luminance range indicate that the performance of warm-white Device 1 is mainly due to the dominant contribution of the G–OR emission, where several advantages of this PPT host–guest system are demonstrated: (i) virtually identical charge-transporting properties, (ii) easily injected energy levels with the HTL/ETL, (iii) well-matched triplet energies of FPPCA and BZQPG, and (iv) the resulting efficient excited energy transfer from FPPCA to BZQPG.<sup>[9]</sup> These factors combine to enable nearly all the electrically generated excitons to be employed for EL emission, leading to the high EL performance. On the other hand, the FPT B–G layer in Device 1, based on a Bepp<sub>2</sub>/FPPCA film with the precisely controlled doping concentration (1.5 wt%) and thickness (10 nm), serves two functions: (i) an extended recombination zone additional to the G–OR layer, where the blue and green emission from direct radiative decay on Bepp<sub>2</sub> and harvesting excitons by FPPCA, respectively, are essential components in the white EL spectrum; (ii) a source of excitons which can diffuse toward the adjacent G–OR layer to sensitize FPPCA molecules, due to their appropriate T<sub>1</sub>-level gradient. This further demonstrates that the free recombination zone consisting of double EMLs without an interlayer in Device 1, which could induce the undesirable charge accumulation as well as the resulting triplet-polaron and/or polaron–polaron quenching processes in the device,<sup>[5c]</sup> allows all the excitons to decay radiatively. The bipolar P molecule FPPCA serves a variety of functions by distributing through both EMLs, is the essential factor for maximizing the overall quantum efficiency, especially to keep high EQE at the high luminance. We have established that the devices reproducibly exhibit the high efficiencies reported, with stable CIE and CRI after continuous operation at a brightness of 1000 cd m<sup>-2</sup> when driven at <4 V for 2–3 h without encapsulation. It should be noted that warm-white light is especially desirable for comfortable ambient lighting that does not cause eye fatigue.<sup>[10]</sup>

In summary, we have reported a warm-white OLED exhibiting EL efficiencies (74.5, 56.5, and 45.8 lm W<sup>-1</sup> and 27.3%, 26.3%, and 24.3%) among the highest reported to date. The CRI is stable (85, 86, and 87) at high and wide-range luminance values of 1000, 5000, and 10 000 cd m<sup>-2</sup>, respectively, utilizing a new-concept emitting system based on the PPT and FPT host–guest combination with a bipolar phosphor FPPCA serving several different roles within two adjacent EMLs. This has enabled not only a simplified device structure and fabrication process but also favorable charge-injecting and energy transfer processes, leading to very high EL performance.

## Supporting Information

Supporting Information is available from the Wiley Online Library or from the author.

## Acknowledgements

M.X.D. and Y.S.F. contributed equally to this work. This work was supported by National Basic Research Program of China (973 Program,

2013CB834805), Natural Science Foundation of China (91333201, 21221063, 51373062, and 51473028), and the key scientific and technological project of Jilin province (20150204011GX). The work at Durham University was supported by EPSRC (the Engineering and Physical Research Council).

Received: January 25, 2016

Revised: March 8, 2016

Published online: May 12, 2016

- [1] a) S. Reineke, F. Lindner, G. Schwartz, N. Seidler, K. Walzer, B. Lüssem, K. Leo, *Nature* **2009**, *459*, 234; b) K. T. Kamtekar, A. P. Monkman, M. R. Bryce, *Adv. Mater.* **2010**, *22*, 572; c) M. C. Gather, A. Köhnen, K. Meerholz, *Adv. Mater.* **2011**, *23*, 233; d) B. W. D'Andrade, S. R. Forrest, *Adv. Mater.* **2004**, *16*, 1585.
- [2] a) S. J. Su, E. Gonmori, H. Sasabe, J. Kido, *Adv. Mater.* **2008**, *20*, 4189; b) R. J. Wang, D. Liu, H. C. Ren, T. Zhang, H. M. Yin, G. Y. Liu, J. Y. Li, *Adv. Mater.* **2011**, *23*, 2823; c) J. Ye, C.-J. Zheng, X.-M. Ou, X.-H. Zhang, M.-K. Fung, C.-S. Lee, *Adv. Mater.* **2012**, *24*, 3410; d) C.-C. Lai, M.-J. Huang, H.-H. Chou, C.-Y. Liao, P. Rajamalli, C.-H. Cheng, *Adv. Funct. Mater.* **2015**, *25*, 5548; e) X. H. Ouyang, X.-L. Li, L. Ai, D. B. Mi, Z. Ge, S.-J. Su, *ACS Appl. Mater. Interfaces* **2015**, *7*, 7869; f) B. Q. Liu, H. Nie, X. B. Zhou, S. B. Hu, D. X. Luo, D. Y. Gao, J. H. Zou, M. Xu, L. Wang, Z. J. Zhao, A. J. Qin, J. B. Peng, H. L. Ning, Y. Cao, B. Z. Tang, *Adv. Funct. Mater.* **2016**, *26*, 776.
- [3] a) Y.-S. Park, J.-W. Kang, D. M. Kang, J.-W. Park, Y.-H. Kim, S.-K. Kwon, S. C. Shin, J.-J. Kim, *Adv. Mater.* **2008**, *20*, 1957; b) C. M. Han, G. H. Xie, H. Xu, Z. S. Zhang, L. H. Xie, Y. Zhao, S. Y. Liu, W. Huang, *Adv. Mater.* **2011**, *23*, 2491; c) C.-J. Zheng, J. Wang, J. Ye, M.-F. Lo, X.-K. Liu, M.-K. Fung, X.-H. Zhang, C.-S. Lee, *Adv. Mater.* **2013**, *25*, 2205.
- [4] a) G. Schwartz, S. Reineke, T. C. Rosenow, K. Walzer, K. Leo, *Adv. Funct. Mater.* **2009**, *19*, 1319; b) J. H. Zou, H. Wu, C.-S. Lam, C. D. Wang, J. Zhu, C. M. Zhong, S. J. Hu, C.-L. Ho, G.-J. Zhou, H. B. Wu, W. C. H. Choy, J. B. Peng, Y. Cao, W.-Y. Wong, *Adv. Mater.* **2011**, *23*, 2976; c) N. Sun, Q. Wang, Y. B. Zhao, Y. H. Chen, D. Z. Yang, F. C. Zhao, J. S. Chen, D. G. Ma, *Adv. Mater.* **2014**, *26*, 1617; d) Z. B. Wu, J. Luo, N. Sun, L. P. Zhu, H. D. Sun, L. Yu, D. Z. Yang, X. F. Qiao, J. S. Chen, C. L. Yang, D. G. Ma, *Adv. Funct. Mater.* **2016**, DOI: 10.1002/adfm.201505602.
- [5] a) Q. Wang, J. Q. Ding, D. G. Ma, Y. X. Cheng, L. X. Wang, F. S. Wang, *Adv. Mater.* **2009**, *21*, 2397; b) H. Sasabe, J.-I. Takamatsu, T. Motoyama, S. Watanabe, G. Wagenblast, N. Langer, O. Molt, E. Fuchs, C. Lennartz, J. Kido, *Adv. Mater.* **2010**, *22*, 5003; c) Y.-L. Chang, S. Yin, Z. B. Wang, M. G. Helander, J. Qiu, L. Chai, Z. W. Liu, G. D. Scholes, Z. H. Lu, *Adv. Funct. Mater.* **2013**, *23*, 705; d) L. P. Zhu, Z. B. Wu, J. S. Chen, D. G. Ma, *J. Mater. Chem. C* **2015**, *3*, 3304; e) Y.-M. Xie, L.-S. Cui, Y. Liu, F.-S. Zu, Q. Li, Z.-Q. Jiang, L.-S. Liao, *J. Mater. Chem. C* **2015**, *3*, 5347; f) Q. Wang, L. W. H. Oswald, X. L. Yang, G. J. Zhou, H. P. Jia, Q. Q. Qiao, J. Hoshikawa-Halbert, B. E. Gnade, *Adv. Electron. Mater.* **2015**, *1*, 1400040.
- [6] a) G. Schwartz, M. Pfeiffer, S. Reineke, K. Walzer, K. Leo, *Adv. Mater.* **2007**, *19*, 3672; b) Y. H. Chen, F. C. Zhao, Y. B. Zhao, J. S. Chen, D. G. Ma, *Org. Electron.* **2012**, *13*, 2807; c) G. Schwartz, S. Reineke, T. C. Rosenow, K. Walzer, K. Leo, *Adv. Funct. Mater.* **2009**, *19*, 1319.
- [7] a) T. Tsuzuki, S. Tokito, *Adv. Mater.* **2007**, *19*, 276; b) Z. Q. Gao, M. Luo, X. H. Sun, H. L. Tam, M. S. Wong, B. X. Mi, P. F. Xia, K. W. Cheah, C. H. Chen, *Adv. Mater.* **2009**, *21*, 688; c) A. Chaskar, H.-F. Chen, K.-T. Wong, *Adv. Mater.* **2011**, *23*, 3876; d) T. Peng, Y. Yang, Y. Liu, D. G. Ma, Z. M. Hou, Y. Wang, *Chem. Commun.* **2011**, *47*, 3150.

- [8] a) Y. Q. Li, Y. Liu, W. M. Bu, D. Lu, Y. Wu, Y. Wang, *Chem. Mater.* **2000**, *12*, 2672; b) Y. Liu, J. H. Guo, J. Feng, H. D. Zhang, Y. Q. Li, Y. Wang, *Appl. Phys. Lett.* **2001**, *78*, 2300; c) T. Peng, Y. Yang, H. Bi, Y. Liu, Z. M. Hou, Y. Wang, *J. Mater. Chem.* **2011**, *21*, 3551.
- [9] G. M. Li, D. X. Zhu, T. Peng, Y. Liu, Y. Wang, M. R. Bryce, *Adv. Funct. Mater.* **2014**, *24*, 7420.
- [10] a) J.-H. Jou, R.-Z. Wu, H.-H. Yu, C.-J. Li, Y.-C. Jou, S.-H. Peng, Y.-L. Chen, C.-T. Chen, S.-M. Shen, P. Joers, C.-Y. Hsieh, *ACS Photonics* **2014**, *1*, 27; b) J. Ye, Z. Chen, F. F. An, M. L. Sun, H.-W. Mo, X. H. Zhang, C.-S. Lee, *ACS Appl. Mater. Interfaces* **2014**, *6*, 8964; c) X.-K. Liu, Z. Chen, J. Qing, W.-J. Zhang, B. Wu, H. L. Tam, F. R. Zhu, X.-H. Zhang, C.-S. Lee, *Adv. Mater.* **2015**, *27*, 7079; d) L.-S. Cui, Y. Liu, X.-Y. Liu, Z.-Q. Jiang, L.-S. Liao, *ACS Appl. Mater. Interfaces* **2015**, *7*, 11007.
- [11] a) Y. C. Zhu, L. Zhou, H. Y. Li, Q. L. Xu, M. Y. Teng, Y. X. Zheng, J. L. Zuo, H. J. Zhang, X. Z. You, *Adv. Mater.* **2011**, *23*, 4041; b) C. Murawski, P. Liehm, K. Leo, M. C. Gather, *Adv. Funct. Mater.* **2014**, *24*, 1117.
- [12] a) Y. Q. Li, M. K. Fung, Z. Y. Xie, S.-T. Lee, L.-S. Hung, J. M. Shi, *Adv. Mater.* **2002**, *14*, 1317; b) K. K. Tsung, S. K. So, *Appl. Phys. Lett.* **2008**, *92*, 103315.
- [13] M. A. Baldo, D. F. O'Brien, M. E. Thompson, S. R. Forrest, *Phys. Rev. B* **1999**, *60*, 14422.
- [14] a) N. Li, S. Oida, G. S. Tulevski, S.-J. Han, J. B. Hannon, D. K. Sadana, T.-C. Chen, *Nat. Commun.* **2013**, *4*, 2294; b) S. Lee, H. Shin, J.-J. Kim, *Adv. Mater.* **2014**, *26*, 5864; c) D. D. Zhang, L. Duan, Y. G. Zhang, M. H. Cai, D. Q. Zhang, Y. Qiu, *Light: Sci. Appl.* **2015**, *4*, e232.
- [15] a) A guide to energy efficient and cost effective lighting, [www.seai.ie](http://www.seai.ie) (accessed: December 2015); b) Lighting technologies: a guide to energy efficient illumination, [www.energystar.gov/ia/partners/promotions/change\\_light/downloads/Fact\\_Sheet\\_Lighting\\_Technologies.pdf](http://www.energystar.gov/ia/partners/promotions/change_light/downloads/Fact_Sheet_Lighting_Technologies.pdf) (accessed: December 2015).